



Open Research Online

The Open University's repository of research publications and other research outputs

Visualising interactions in bi- and triadditive models for three-way tables

Journal Item

How to cite:

Albers, Casper and Gower, John (2017). Visualising interactions in bi- and triadditive models for three-way tables. *Chemometrics and Intelligent Laboratory Systems*, 167 pp. 238–247.

For guidance on citations see [FAQs](#).

© 2017 The Authors

Version: Accepted Manuscript

Link(s) to article on publisher's website:

<http://dx.doi.org/doi:10.1016/j.chemolab.2017.05.014>

<http://doi.org/10.1016/j.chemolab.2017.05.014>

Copyright and Moral Rights for the articles on this site are retained by the individual authors and/or other copyright owners. For more information on Open Research Online's data [policy](#) on reuse of materials please consult the policies page.

oro.open.ac.uk

Accepted Manuscript

Visualising interactions in bi- and triadditive models for three-way tables

Casper Albers, John Gower

PII: S0169-7439(17)30323-4

DOI: [10.1016/j.chemolab.2017.05.014](https://doi.org/10.1016/j.chemolab.2017.05.014)

Reference: CHEMOM 3445

To appear in: *Chemometrics and Intelligent Laboratory Systems*

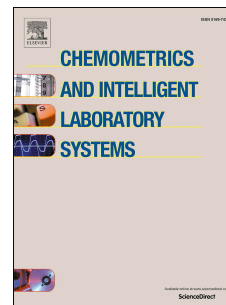
Received Date: 3 September 2015

Revised Date: 12 May 2017

Accepted Date: 15 May 2017

Please cite this article as: C. Albers, J. Gower, Visualising interactions in bi- and triadditive models for three-way tables, *Chemometrics and Intelligent Laboratory Systems* (2017), doi: 10.1016/j.chemolab.2017.05.014.

This is a PDF file of an unedited manuscript that has been accepted for publication. As a service to our customers we are providing this early version of the manuscript. The manuscript will undergo copyediting, typesetting, and review of the resulting proof before it is published in its final form. Please note that during the production process errors may be discovered which could affect the content, and all legal disclaimers that apply to the journal pertain.



Visualising interactions in bi- and triadditive models for three-way tables

Casper Albers* John Gower†

May 16, 2017

Abstract

This paper concerns the visualisation of interaction in three-way arrays. It extends some standard ways of visualising biadditive modelling for two-way data to the case of three-way data. Three-way interaction is modelled by the Parafac method as applied to interaction arrays that have main effects and biadditive terms removed. These interactions are visualised in three and two dimensions. We introduce some ideas to reduce visual overload that can occur when the data array has many entries. Details are given on the interpretation of a novel way of representing rank-three interactions accurately in two dimensions. The discussion has implications regarding interpreting the concept of interaction in three-way arrays.

Keywords. Interpretation of interaction, Modelling of interaction, Visualisation of interaction, Biadditive Models, Individual Scaling.

*Department of Psychometrics & Statistics, University of Groningen, Groningen, The Netherlands; corresponding author, c.j.albers@rug.nl.

†Department of Mathematics & Statistics, The Open University, Milton Keynes, United Kingdom.

1 Setting the scene

“...It is important that the final model or models should make sense physically: at a minimum, this usually means that interactions should not be included without main effects nor higher-degree polynomial terms without their lower-degree relatives. Furthermore, if the model is to be used as a summary of the findings of one out of several studies bearing on the same phenomenon, main effects would usually be included whether significant or not. Strict adherence to this policy makes it easier to compare the results of various studies and helps to avoid the apparent conflicts that occur when different fitted models with different sets of terms are used in each study.”

McCullagh and Nelder (1989, p.89)

In this paper, we are concerned with three-way tables \mathbf{X} with elements x_{ijk} ($i = 1, \dots, I$; $j = 1, \dots, J$; $k = 1, \dots, K$). Thus, the factors used to classify the three ways have equal status (sometimes called modes) while the body of the table contains values of a quantitative variable that may be regarded as a dependent variable - as classically typified by a three-way table arising from agricultural experiments with fertilizer treatments as factors and crop yield as the response. The factors are treated as categorical variables but if they happen to have numerical values, this may be taken into account when interpreting interactions. The primary emphasis is on the visualisation of interaction with a supplementary interest in estimation and interpretation seen in the light of the quotation from McCullagh and Nelder (1989). To dispel any suggestion to the contrary, we emphasize that the quotation is not an expression of a mathematical fact but more an observation on how data can usually be expected to behave. In the psychometric literature, a three-way table is sometimes referred to as one-mode three-way data (Carroll and Arabie, 1980; Coombs, 1964; Kiers, 2000) or, shorter, as (data) array, whereas in chemometrics the terminology tensor for \mathbf{X} is more common.

Three-way tables are usually analysed by linear models containing additive terms representing main effects, two-factor interactions, and three-factor interactions. The number of factors can be readily extended to any number of “ways”. The form of such models readily respects the McCullagh and Nelder (1989) quotation. Note that with a dependent interval variable there is a fundamental need for at least one additive parameter to represent translation (e.g. Celsius to Fahrenheit).

For reference, and to establish notation, we list the basic results for additive models. The model is

$$x_{ijk} = m + \{a_i + b_j + c_k\} + \{d_{jk} + e_{ik} + f_{ij}\} + g_{ijk} \quad (1)$$

35 where the terms with a single suffix represent main effects, those with double suffices two
 36 factor interactions and g_{ijk} represents contributions from three factor interactions. Some
 37 components of the interactions may be regarded as “error”. The estimating equations
 38 are subsumed in the identity:

$$\begin{aligned} \hat{x}_{ijk} = & x_{...} + \{(x_{i..} - x_{...}) + (x_{.j.} - x_{...}) + (x_{..k} - x_{...})\} \\ & + \{(x_{.jk} - x_{.j.} - x_{..k} + x_{...}) + (x_{i.k} - x_{i..} - x_{.k.} + x_{...}) \\ & + (x_{ij.} - x_{i..} - x_{.j.} + x_{...})\} \\ & + (x_{ijk} - x_{.jk} + x_{i.k} + x_{ij.} + x_{i..} + x_{.j.} + x_{..k} - x_{...}) \end{aligned} \quad (2)$$

39 where the expressions in braces in (2) estimate the corresponding parameters in (1).
 40 Note that we adopt the convention that a “hat” on the left-hand-side implies that the
 41 terms on the right-hand-side are parameter estimates, else they are the parameters
 42 themselves. The terms in (2) contribute to an orthogonal analysis of variance:

$$\sum_{i,j,k}^{I,J,K} (\hat{x}_{ijk} - x_{...})^2 = JK\|\mathbf{a}\|^2 + IK\|\mathbf{b}\|^2 + IJ\|\mathbf{c}\|^2 + I\|\mathbf{D}\|^2 + J\|\mathbf{E}\|^2 + K\|\mathbf{F}\|^2 + \|\mathbf{G}\|^2 \quad (3)$$

43 where $\mathbf{a}, \mathbf{b}, \mathbf{c}$ are vectors of the main effects, $\mathbf{D}, \mathbf{E}, \mathbf{F}$ are matrices of the two-factor
 44 interactions and $\|\mathbf{G}\|^2$ represents the sum-of-squares of the elements of the three-factor
 45 interaction.

46 When interactions have been estimated, there remains the problem of their inter-
 47 pretation. The terms in (2) represent overall contributions to each main effect and
 48 interaction. To help interpret overall representations of interaction, several simple ap-
 49 proximations have been proposed. One possibility is to focus on the larger (positive or
 50 negative) terms. Another is to fit linear and quadratic polynomials to get, for exam-
 51 ple, linear \times linear \times quadratic estimates. Even the simpler of these can be difficult
 52 to interpret and, strictly speaking, such expressions are valid only when the classifying
 53 factors are numerical (like levels of fertilizer applications).

54 Another possibility is to fit product terms like $a_i b_j$. Products of two factors have
 55 bilinear regression interpretations and a nice geometrical representation that underpins
 56 useful visualisations of two-factor interaction. This possibility of biadditive modelling is
 57 discussed in Section 2. A biadditive model gives the best rank- r least-squares approxi-
 58 mation to a two-way table/matrix but this optimal mathematical property should not
 59 necessarily be taken as an expression of an appeal to underlying substantive multiplica-
 60 tive effects.

61 In a parallel literature, models for analysing three-way data (summarised in Kroonen-
62 berg, 2008; Smilde et al., 2004) often include triple product terms like $a_i b_j c_k$. Included
63 are three-mode principal component analysis (Tucker, 1966) and methods as the Can-
64 decomp (Carroll and Chang, 1970) and Parafac models (Harshman, 1970) (both models
65 are equivalent and commonly denoted as the CP-model). A desirable computational
66 requirement for fitting three-way multiplicative models is a universal algorithm for fit-
67 ting a general canonical decomposition for three-way arrays. Such models are discussed
68 in Section 3. It is clear that triple product terms may be potentially useful in many
69 contexts and considered as a natural extension for representing triadditive interactions
70 in a similar way that biadditive models may represent two-factor interactions.

71 In many psychometric and chemometric methods, the triple product term domi-
72 nates the model, even to the extent of excluding lower order terms, thus not respecting
73 the maxim of McCullagh and Nelder (1989) cited at the start of this paper. This is
74 because in psychometrics the methods are intended as generalisations of Principal Com-
75 ponent Analysis and related methods that do not admit a dependent variable; such
76 methods are beyond the scope of this paper. Nevertheless, triadditive terms may be
77 used to approximate three-way interactions. In the following we exploit the fact that
78 the Candecomp-Parafac algorithm can be useful for fitting three-way multiplicative in-
79 teractions in three-way models. We explore the consequences for the McCullagh and
80 Nelder dictum if this route is taken. Visualisation is important in the interpretation
81 of biadditive interactions and we provide suggestions for its improvement: Appendix A
82 discusses how to calibrate axes Appendix B provides details on optimising a parallel axis
83 display of the interactions and Section 4 demonstrates these methods. Furthermore, we
84 show how triadditive terms may be visualised and interpreted.

85 In the above, we have regarded the overall main effects and interaction terms in (2)
86 as the definitive expressions of interaction. These may then be approximated as we have
87 described, by linear, biadditive or triadditive estimates, perhaps including other parts
88 of the interactions in an error term. For linear and biadditive estimates the procedure
89 of estimating the biadditive part of each interaction, conditionally on the usual least-
90 squares estimates of the linear part, usually turns out to be equivalent to unconditional
91 estimation. However, this is not true for some of the biadditive models we discuss below
92 and for triadditive models it is never true.

93 Sections 2 and 3 briefly summarise some of the current insights in biadditive and
94 triadditive models and discuss various ways of modelling and interpreting interactions
95 using these models. These sections are not meant provide an exhaustive and complete
96 overview of all knowledge on biadditive and triadditive models, as good sources for that
97 already exist (Smilde et al., 2004; Kroonenberg, 2008). Subsequently, biadditive and

98 triadditive visualisations are constructed for an example from agricultural (Section 4)
 99 research. Although these visualisations are based on the Candecom-model Carroll and
 100 Chang (1970), the visualisations can also be based on other techniques for analysing
 101 three-way arrays. Section 5 concludes the paper.

102 2 Biadditive models

103 In this section we summarise well-known results for biadditive models. This establishes
 104 notation that is needed for similar developments with triadditive models discussed in
 105 Section 3.

106 2.1 Biadditive models for two-way tables

107 For an $I \times J$ table \mathbf{X} with elements x_{ij} the general biadditive model is:

$$x_{ij} = m + a_i + b_j + \sum_{r=1}^R c_{ir} \tilde{c}_{jr} + \varepsilon_{ij} \quad (i = 1, \dots, I, j = 1, \dots, J) \quad (4)$$

108 where a_i and b_j represent row and column main effects, and c_{ir} and \tilde{c}_{jr} ($r = 1, \dots, R$)
 109 model the multiplicative interaction. The error terms ε_{ij} are assumed to be indepen-
 110 dently distributed with equal variances. Many classical models, such as Tukey's model
 111 for one degree of freedom for non-additivity (Tukey, 1949), can be considered as spe-
 112 cial cases of a biadditive model. Alternative names under which (4) has appeared, are
 113 FANOVA (FActor ANalysis Of VAriance) (Gollob, 1968) and AMMI (Additive Main
 114 effects and Multiplicative Interactions) (Gauch, 1992). Also the GEMANOVA (Gener-
 115 alised multiplicative ANOVA) model (cf. Bro and Jakobsen, 2002) is related. We prefer
 116 the neutral biadditive model terminology which is in line with general statistical usage
 117 (Denis and Gower, 1994). These authors were interested in biadditivity because they
 118 thought that substantive genetic effects were better modelled in multiplicative rather
 119 than additive terms.

120 In general, model (4) is not fully identified. The simplest identification constraints
 121 for the general model are

$$\left. \begin{aligned} \mathbf{1}'\mathbf{a} = \mathbf{1}'\mathbf{b} = \mathbf{1}'\mathbf{c}_r = \mathbf{1}\tilde{\mathbf{c}}_r = 0 \\ \tilde{\mathbf{c}}_r'\tilde{\mathbf{c}}_r = \mathbf{c}_r'\mathbf{c}_r = \sigma_r, \text{ say, and } \tilde{\mathbf{c}}_r'\tilde{\mathbf{c}}_s = \mathbf{c}_r'\mathbf{c}_s = 0 \quad (r \neq s) \end{aligned} \right\} (r, s = 1, \dots, R) \quad (5)$$

122 ensuring that the matrix $\sum_{r=1}^R c_{ir} \tilde{c}_{jr}$ of interaction parameters of rank R is uniquely
 123 parameterised in the form of its singular value decomposition with singular values

124 $\sigma_1, \dots, \sigma_R$.

125 The analysis of variance corresponding to a two-way version of (4) is:

$$\sum_{i,j}^{I,J} (\hat{x}_{ij} - x_{..})^2 = J\|\mathbf{a}\|^2 + I\|\mathbf{b}\|^2 + \sum_{r=1}^R \sigma_r^2 + \sum_{r=R+1}^{\rho} \sigma_r^2 \quad (6)$$

126 where $\rho = \text{rank}(\mathbf{X})$.

127 2.2 Biadditive models for three-way tables

128 Biadditive terms may be used to model interaction in three-way tables (cf. Gower, 1977).

129 For an $I \times J \times K$ table \mathbf{X} with elements x_{ijk} we may consider the following biadditive
130 model:

$$x_{ijk} = m + a_i + b_j + c_k + \sum_{p=1}^P d_{jp} \tilde{d}_{kp} + \sum_{q=1}^Q e_{iq} \tilde{e}_{kq} + \sum_{r=1}^R f_{ir} \tilde{f}_{jr} + \varepsilon_{ijk} \quad (7)$$

131 for $i = 1, \dots, I; j = 1, \dots, J; k = 1, \dots, K$, where the ε_{ijk} are the elements of the
132 three-way error array \mathbf{E} .

133 Similar identification constraints to those already discussed for model (4) may be
134 applied for the biadditive model (7) for three-way tables:

$$\mathbf{1}'\mathbf{a} = \mathbf{1}'\mathbf{b} = \mathbf{1}'\mathbf{c} = \mathbf{1}'\mathbf{d}_p = \mathbf{1}'\tilde{\mathbf{d}}_p = \mathbf{1}'\mathbf{e}_q = \mathbf{1}'\tilde{\mathbf{e}}_q = \mathbf{1}'\mathbf{f}_r = \mathbf{1}'\tilde{\mathbf{f}}_r = 0$$

135 for $p = 1, \dots, P; q = 1, \dots, Q; r = 1, \dots, R$, together with the SVDs of the three
136 biadditive interaction matrices as they occur in (2). The resulting analysis of variance
137 is:

$$\sum_{i,j,k=1}^{I,J,K} (\hat{x}_{ijk} - x_{...})^2 = JK\|\mathbf{a}\|^2 + IK\|\mathbf{b}\|^2 + IJ\|\mathbf{c}\|^2 + I \sum_{s=1}^P \sigma_{ps}^2 + J \sum_{s=1}^Q \sigma_{qs}^2 + K \sum_{s=1}^R \sigma_{rs}^2 + \sigma^2 \quad (8)$$

138 where the singular values σ_{ps} ($s = 1, \dots, P$), σ_{qs} ($s = 1, \dots, Q$) and σ_{rs} ($s = 1, \dots, R$)
139 refer to the respective residual tables \mathbf{Z}_i , \mathbf{Z}_j and \mathbf{Z}_k defined as in (2), and σ^2 is the
140 residual sum-of-squares obtained from all the singular values not included in the sum-
141 mations. The solution for the multiplicative constants is then obtained from the SVD
142 of the two-way tables of residuals \mathbf{Z}_i , \mathbf{Z}_j and \mathbf{Z}_k . This is a simple generalisation that
143 may be readily extended to tables of any number of “ways”.

144 The choice of ranks P , Q and R can be made by ad hoc arguments, such as that
145 rank 2 approximations can be visualised and communicated in an understandable way.

146 Another option lies in more formal arguments such as obtaining corresponding degrees
 147 of freedom, for instance for the $A \times B$ interaction, through the rule of thumb that (i)
 148 degrees of freedom for $P = 1, 2, \dots, \min(I - 1, J - 1)$ should add up to that of the $A \times B$
 149 interaction in the two-way ANOVA table, (ii) the df for dimension i should be two less
 150 than that for dimension $i - 1$. According to (Gower et al., 2011, Section 6.3), this rule
 151 was first given by Rao (1952). A formal test of significance for P , Q or $R = 1$ has been
 152 given by Corsten and Eijnsbergen (1972). Other approaches include cross-validation
 153 and using multiway extensions of the Kaiser criterion or scree plot (Kroonenberg and
 154 van der Voort, 1987), such as the DifFit procedure for Tucker3 models (Timmerman
 155 and Kiers, 2000). See Smilde et al. (2004, Section 7.4) and Kroonenberg (2008, Section
 156 8.5) for an overview of component-selection methods.

157 2.3 Visualisation for biadditive models

158 It is useful, especially when $R = 2$, to plot the rows of \mathbf{c}_r ($r = 1, \dots, R$) to give I
 159 row-points and the rows of $\tilde{\mathbf{c}}_r$ ($r = 1, \dots, R$) to give J column-points. In this biplot, the
 160 inner-product determined by a pair of points, one from each set, gives a visualisation of
 161 the corresponding interaction. This is a well-known form of biplot (see e.g. Gower et al.,
 162 2011). Another possibility is to present the rows as axes and the columns as points
 163 (or vice versa). The axes may be calibrated, making it trivial to find values of inner
 164 products.

165 Furthermore, axes may include markers for the row or column main effects. As
 166 we show in Appendix A, calibrated axes may be provided *simultaneously* for rows and
 167 columns *and* both sets of main effects may be included. In addition, the values of
 168 $\alpha + \beta = 1$ (as defined in Appendix A) are at choice and λ -scaling is available (see
 169 Gower et al., 2011). In this way, a variety of equivalent representations, which may be
 170 regarded as items drawn from a toolbox, is available for presentational purposes. One
 171 may choose among the possibilities to represent only the more important interactions.
 172 Some examples are included in Section 4 of this paper.

173 The biplot representation of two-factor interactions is an attractive aid to interpre-
 174 tation. Also the biadditive model of three-way data can be visualised, now by three
 175 biplots, one for each biadditive term in (7).

176 3 Triadditive models

177 3.1 Triadditive models for three-way data

178 For an $I \times J \times K$ table $\underline{\mathbf{X}}$ with elements x_{ijk} , consider the following triadditive model:

$$x_{ijk} = m + a_i + b_j + c_k + \sum_{p=1}^P d_{jp} \tilde{d}_{kp} + \sum_{q=1}^Q e_{iq} \tilde{e}_{kq} + \sum_{r=1}^R f_{ir} \tilde{f}_{jr} + \sum_{s=1}^S g_{is} \tilde{g}_{js} \tilde{g}_{ks} + \varepsilon_{ijk} \quad (9)$$

179 This model is an extension of (7) where the error array $\underline{\mathbf{E}}$ is partitioned into a rank- S
 180 triadditive part $\underline{\mathbf{G}}$ and a new error array $\underline{\mathbf{E}}$ with, generally, a smaller sum of squared
 181 elements than that of (7). For identification, the usual zero-sum identification constraints
 182 may be applied to all the parameters but when applied to the triadditive parameters
 183 g_{is} , \tilde{g}_{js} , \tilde{g}_{ks} it has unexpected implications. This is because adding constants α , β , γ
 184 replaces the triadditive term by $(g_{is} + \alpha)(\tilde{g}_{js} + \beta)(\tilde{g}_{ks} + \gamma)$ which, on expansion, induces
 185 additional additive and biadditive terms. The additive terms may be absorbed into
 186 zero-sum main effects without affecting the form of the model. This is not so for the
 187 biadditive terms, where unabsorbable parts of the triadditive interaction contribute to
 188 the biadditive parameters, thus increasing their rank. Thus, this reparameterisation
 189 changes the form of the model. One consequence is that the least-squares estimates
 190 of the triadditive interaction parameters are not the same as the estimates conditional
 191 on the estimated main effects and biadditive interactions. Another, is that the usual
 192 orthogonal analysis of variance is not available. This position may be accepted and
 193 algorithms developed to fit the model but a more simple option is to fit the triadditive
 194 part conditional on the main effects and the saturated biadditive component of the
 195 model. That is, we fit the triadditive part of the model to the biadditive residual table:

$$\hat{z}_{ijk} = x_{ijk} - x_{.jk} - x_{i.k} - x_{ij.} + x_{i..} + x_{.j.} + x_{..k} - x_{...} \quad (10)$$

196 Triadditive interactions in (9) may be modelled in two ways. If z_{ijk} represents a
 197 typical term of the interaction we may fix one factor, say i , and consider the I
 198 way tables $\{z_{1jk}\}, \{z_{2jk}\}, \dots, \{z_{Ijk}\}$. Each of these tables may be fitted by a biadditive
 199 model and the results compared. This approach is consistent with the classical notion
 200 of interaction as a difference in response to a factor, or set of factors (here j and k), at
 201 different levels of another factor (here i). Of course, we may interchange the roles of i , j
 202 and k . The other approach is to fit a truly triadic model with the Candecomp-Parafac

203 algorithm (Carroll and Chang, 1970; Harshman, 1970), minimising:

$$\sum_{i,j,k=1}^{I,J,K} \sum_{r=1}^R (z_{ijk} - u_{ir}v_{jr}w_{kr})^2. \quad (11)$$

204 We choose for this approach as it is a truly triadic approach. The approximation (11)
 205 may be viewed as the triadditive counterpart of the Eckart-Young theorem but lacking
 206 a nice known canonical decomposition. (See also Schmidt (1907), which is said to be
 207 the first example of the SVD least-squares property, albeit in a very different field from
 208 data analysis.) This approach is close to the classical approximation of interactions
 209 by orthogonal polynomials in linear models. Here we fit a biadditive approximation to
 210 the two-way interactions and a triadditive approximation to the three-way interaction
 211 terms of (1) and (2). The residuals from the triadic term contribute to the term (11),
 212 while the biadditive part contributes components what we denote by σ^2 in (8). In a
 213 good fit, these two components should be comparable giving some indication of stability
 214 and, when available, they may be compared with independent estimates of replication-
 215 error. From the statistical point of view we need some concept akin to that of degrees
 216 of freedom in linear models. What is known about this is summarised by Kroonenberg
 217 (2008, Section 8.4). Related to this is the concept of rank for three-way arrays (cf. ten
 218 Berge (2011) and Smilde et al. (2004, Section 2.6)). Triadditive rank is defined as the
 219 smallest value of R that gives an exact triadditive fit. The interaction array \mathbf{Z} , with its
 220 zero marginals, generally has lower rank than the data array \mathbf{X} (Albers et al., 2017).
 221 Since our focus lies on the visualisation of interactions, here we will not formally study
 222 rank properties of \mathbf{Z} .

223 3.2 Visualisation for three-way data

224 As with the biadditive model, when a rank R triadic model (11) has been fitted, there
 225 is interest in expressing the interaction in graphical form. In the rank one case ($R = 1$),
 226 the points for u_{i1} ($i = 1, \dots, I$); v_{j1} ($j = 1, \dots, J$); w_{k1} ($k = 1, \dots, K$) may be placed on
 227 separate orthogonal coordinate axes, which we shall label u , v and w . Then, $u_{i1}v_{j1}w_{k1}$
 228 is simply proportional to the volume of the tetrahedron with these three points on
 229 orthogonal *axes* and the origin as vertices (Figure 1, left).

230 When $R = 2$, the visualisation remains basically Euclidean in three dimensions and it
 231 may be interpreted in terms of tetrahedral volume where the vertices of the tetrahedra
 232 are confined to the origin and three orthogonal *planes* (Figure 1, right). The justification

233 of this approach follows from the trilinear identity:

$$\det \begin{pmatrix} 0 & u_{i1} & u_{i2} \\ v_{j2} & 0 & v_{j1} \\ w_{k1} & w_{k2} & 0 \end{pmatrix} = u_{i1}v_{j1}w_{k1} + u_{i2}v_{j2}w_{k2} \quad (12)$$

234 (see also equation (4) in Albers and Gower (2014)). The rows of the determinant on
 235 the left hand side may be interpreted as giving the coordinates of three points, one in
 236 each of three orthogonal dimensions, while the right hand side gives a term in the rank
 237 two triadditive model. Albers and Gower (2014) give further details and show that,
 238 without loss of information, this representation may be shown in two dimensions to give
 239 a visualisation which resembles a biplot, with one set of K coplanar points and two sets of
 240 calibrated axes representing the remaining IJ factors. Thus, it is a ‘triplot’ rather than a
 241 biplot (see e.g. Gower et al., 2011). Whilst Albers and Gower (2014) explain the technical
 242 construction of these triplots, instruction on how to interpret these triplots, especially
 243 in the case of interaction arrays, is lacking. We provide such explanation Section 4.
 244 That rank-two trilinear interactions may be shown in two dimensions, gives them similar
 245 status to interactions for bilinear models and makes direct three-dimensional tetrahedral
 246 visualisations unnecessary. We believe that this is a major step forward.

247 * FIGURE 1 ABOUT HERE *

248 Because volume is invariant to orthogonal transformations, one may deduce from the
 249 above three-dimensional representation that the parameters of rank 2 triadditive models
 250 are determined only up to arbitrary orthogonal rotations in three dimensions. This de-
 251 gree of arbitrariness is similar to that found in biadditive models where inner-products or,
 252 equivalently, areas (Gower et al., 2010) rather than volume are the invariants. Orthog-
 253 onal transformation is not the only invariant for rank 2 triadditive models; for example,
 254 provided $\alpha\beta\gamma = 1$, we could also scale the three axes by α , β , γ , respectively, without
 255 affecting volume. Our experience is that visualisation that yields easiest interpretation
 256 is achieved when α , β and γ are chosen such that $\sum_{i,r} u_{i,r}^2 \approx \sum_{j,r} v_{j,r}^2 \approx \sum_{k,r} w_{k,r}^2$.
 257 With this degree of arbitrariness, we see little point in paying much attention to the
 258 estimated values of the parameters u , v , w but rather to focus on the invariants, such
 259 as volume and the actual fitted values \hat{x}_{ijk} and \hat{z}_{ijk} .

260 Higher rank solutions to biadditive models can be shown as three-dimensional images
 261 or by exhibiting several planar cross-sections of the higher-dimensional space. Neither
 262 of these is satisfactory and it is the two-dimensional approximations that are by far the
 263 most important. Nevertheless, it is interesting to see what progress can be made with

264 representing triadditive terms for $R = 3$. We could show this as three volumes, each of
 265 unit rank $(u_{i1}v_{j1}w_{k1}) + (u_{i2}v_{j2}w_{k2}) + (u_{i3}v_{j3}w_{k3})$, or of two volumes, one of unit rank
 266 and the other of rank two $(u_{i1}v_{j1}w_{k1}) + (u_{i2}v_{j2}w_{k2} + u_{i3}v_{j3}w_{k3})$. A more symmetric
 267 representation arises from noting that

$$2(u_{i1}v_{j1}w_{k1} + u_{i2}v_{j2}w_{k2} + u_{i3}v_{j3}w_{k3}) \quad (13)$$

$$= \det \begin{pmatrix} 0 & u_{i1} & u_{i2} \\ v_{j2} & 0 & v_{j1} \\ w_{k1} & w_{k2} & 0 \end{pmatrix} + \det \begin{pmatrix} 0 & u_{i1} & u_{i3} \\ v_{j3} & 0 & v_{j1} \\ w_{k1} & w_{k3} & 0 \end{pmatrix} + \det \begin{pmatrix} 0 & u_{i2} & u_{i3} \\ v_{j3} & 0 & v_{j2} \\ w_{k2} & w_{k3} & 0 \end{pmatrix}.$$

268 After equation (12), we explained how this determinant is equal to the volume of a single
 269 tetrahedron. Using analogous arguments, equation (13) equals three times the sum of
 270 the volumes of the tetrahedra designated by the three separate determinants. We have
 271 seen that when $R = 1$, the three axes share a common origin and when $R = 2$ the
 272 three planes share an orthogonal set of axes. When $R = 3$ we retain the orthogonal
 273 axes u, v, w but, as is shown by (13), it is the projections of the points $(u_{i1}u_{i2}u_{i3})$,
 274 $(v_{j1}v_{j2}v_{j3})$, (w_{k1}, w_{k2}, w_{k3}) onto the (vw) , (wu) , (uv) planes that determine the vertices
 275 of the operative tetrahedra. The display of Figure 2 shows that this visualisation is on
 276 the boundary of what is relevant for practical purposes.

277 Interestingly, when $R = 4$ we may write $(u_{i1}v_{j1}w_{k1} + u_{i2}v_{j2}w_{k2}) + (u_{i3}v_{j3}w_{k3} +$
 278 $u_{i4}v_{j4}w_{k4})$ the sum of two rank 2 terms each representable by a single tetrahedron.
 279 However, adding even two volumes is not acceptable. We conclude that rank two rep-
 280 resentations of triadditive models are at the limits of useful graphical representation;
 281 higher ranks are possible but are impracticable.

282 * FIGURE 2 ABOUT HERE *

283 4 Application: response of wheat varieties to the ap- 284 plication of nitrogen fertiliser at different sites

285 Blackman et al. (1978) studied the effect of the application of nitrogen fertiliser to several
 286 varieties of winter wheat of contrasting height grown at different trial sites. The data
 287 consists of a fully crossed design with the following three factors:

- 288 A Rate of nitrogen application ($I = 2$ levels, low and high)
- 289 B Trial sites ($J = 7$ locations in the United Kingdom)
- 290 C Variety ($K = 12$ different varieties).

291 The names of the factor levels for factors B and C are given in Table 1. A fourth
 292 factor, indicating whether the variety is either ‘conventional’ (varieties Cappelle, Ranger,
 293 Huntsman, Templar, and Kinsman) or ‘semi-dwarf’ (varieties Fundin, Durin, Hobbit,
 294 Sportsman, TJB295/95, TJB325/464, and Hustler), is excluded from our analysis as it’s
 295 obviously not a crossed factor. The dependent variable is grain yield, measured in grams
 296 per square meter. One trial site (Edinburgh) is located in Scotland, the six others are
 297 all located in Cambridgeshire and Oxfordshire, England. In this section we are mainly
 298 concerned with visual presentation of interactions rather than with substantive analysis.

299 4.1 Biadditive visualisation

300 First, we fit the biadditive model as outlined in Section 2.2. Table 2 shows that factor
 301 B, Trial Site, is the most important main factor and the interaction between A, rate of
 302 nitrogen application, and B is the most important two-way interaction. The main effects
 303 constitute 84% of total variation in grain yield, the two-way interactions 14% and the
 304 three-way interaction 2%.

305 Table 2 also provides the sums-of-squares of the low-rank approximations to the two-
 306 way interaction between B and C, according to Equation (7) with approximations to
 307 degrees of freedom as suggested by Rao (1952) (see Section 2.2). Since Factor A has
 308 two levels, $df_A = 1$. Hence, this low-rank approximation does not apply to the AB
 309 and AC interactions: the full-rank approximation is already of the lowest rank possible.
 310 Were $df_A > 1$, the treatment of the low-rank approximations to interactions AB and
 311 AC would have been analogous to that of BC. Corresponding to BC, most information,
 312 79%, is captured in the first two dimensions.

313 For this data, two-dimensional biplots of interactions with factor A are not relevant:
 314 A has only two levels, thus the interactions are one-dimensional. Figure 3 gives a series
 315 of equivalent biplots for interaction BC. In all cases, interpretation is through evaluating
 316 inner-products, either directly or indirectly. Figure 3a visualises the interaction BC in
 317 the conventional way. Often, the points are connected to the origin and perhaps endowed
 318 with arrows. The interactions of the varieties at the trial site in Edinburgh clearly deviate
 319 from those at the six English sites. A closer examination confirms that the McCullagh
 320 and Nelder dictum, cited at the beginning of this paper, holds. Interestingly, no clear
 321 distinction in interaction can be found between the regular and the semi-dwarf varieties.

322 Figure 3a is useful for assessing global patterns in the data but no numerical values
 323 can be read off. For this, calibrated axes are needed. The technicalities behind the
 324 construction of such axes simultaneously for sites and varieties is explained in Appendix
 325 A. The biplots in the other panels make use of such calibrated axes. They give the same

326 information as Figure 3a, but in 3b and 3c, while varieties continue to be represented by
 327 points, trial sites are represented by calibrated axes. The Figures show exclusion (3b)
 328 vs. inclusion (3c) of main effects but otherwise are identical; thus Figure 3b displays
 329 the biadditive interactions *after* the main effects have been partialled out, whereas these
 330 are still included in Figure 3c. The only difference between panels (b) and (c) is the
 331 calibration of the axes: where in panel (b) all axes have value 0 at the origin, this
 332 is not the case in panel (c). Figure (3d) shows calibrated axes for both varieties and
 333 sites. Note that a variety projected onto a site-axis gives the same calibration as the
 334 same site projected onto the corresponding variety axis. For example, consider variety
 335 Sportsman and site Edinburgh (as shown in Figure 3(d)): The projection of Sportsman
 336 onto Edinburgh is -30.33 g/sqm, which is equivalent to the projection of Edinburgh onto
 337 Sportsman. The same holds for all other pairs of sites and varieties.

338 * TABLES 1 & 2, FIGURES 3 & 4 ABOUT HERE *

339 Thus, with Figure 3(a) inner products are not needed to rank varieties *within* a site or
 340 to rank sites growing the same variety but it is difficult to make numerical comparisons
 341 *between* sites and varieties. This problem is reduced by using the calibrations in Figure
 342 3(b) and Figure 3(c) but the calibration markers tend to lead to problems of visual
 343 overload.

344 Figure 4 is a compromise which preserves most of the useful information and is easy
 345 to use. Essentially, it consists of taking the axes of one set of calibrations (say, the seven
 346 sites) and laying them horizontally on successive lines with a common origin in a so-
 347 called parallel coordinate plot (cf. Inselberg, 2009). The different interval of calibration
 348 on each axis will be clear and can be removed by normalising each line to have an equal
 349 interval of calibration. Then, the calibration markers on the successive lines can be
 350 removed and replaced by a single calibrated axis applicable to all sites, as shown in
 351 Figure 4. Parallel coordinate plots date back to (at least) the 17th century (d’Ocagne,
 352 1885) and gained popularity through the work of Inselberg in the past four decades
 353 (Inselberg, 2009). The usage of parallel coordinate plots in the context of three-way
 354 analysis is not new (cf. Kroonenberg, 2008, p. 400), but this paper is, to our knowledge,
 355 the first that employs parallel coordinate plots to visualise three-way interactions.

356 In this example, there is no logical ordering for the sites. Rather than the alphabet-
 357 ical ordering in Figure 4, any other of the $J! = 5040$ orderings can be used. Although
 358 all variations provide exactly the same information, some allow for easier interpretation
 359 because there is less ‘clutter’, such as fewer line-crossings. When J is not too large,
 360 one can resort to manual reordering but for larger values of J , an automated proce-
 361 dure is preferable. We propose such a procedure, based on correspondence analysis (cf.

362 Greenacre, 2007). Technicalities of this procedure are provided in Appendix B and Fig-
 363 ure 5 shows the optimal ordering. This figure provides *exactly* the same information as
 364 Figure 4 but is easier to interpret.

365 Now, the performance of every variety at each site may be readily compared directly.
 366 The main effects may be included if desired but we have not done this with these data
 367 because of the disproportionate main effect of Edinburgh (a value +232 grams per square
 368 meter; whereas the other six sites have main effects between -113 and $+46$ grams per
 369 square meter). Of course, an equivalent procedure can be used for the varieties rather
 370 than for the sites.

371 4.2 Triadditive visualisation

372 Having eliminated all main and multiplicative effects according to (10), Candecom-
 373 Parafac approximations of different rank were fitted to $\hat{\mathbf{Z}}$. Table 3 displays the break-
 374 down of the ABC-interaction SS of 49812 into approximations of rank 1 to 6. Rank 2
 375 and 3 approximation explain 63% and 78% of the variation in grain yield, respectively.
 376 Thus, visualisations on the basis of these approximations will yield useful insight into
 377 the structure of $\hat{\mathbf{Z}}$.

378 Figure 1 visualises the rank 1 and 2 approximations to the three-way interaction
 379 term. The highlighted interaction in each figure is that between a low rate of nitrogen
 380 application, trial site Edinburgh variety Kinsmen. The data have been scaled by α , β ,
 381 and γ in such a way that

$$\sum_{i=1}^I \sum_{r=1}^R u_{ir}^2 = \sum_{j=1}^J \sum_{r=1}^R v_{jr}^2 = \sum_{k=1}^K \sum_{r=1}^R w_{kr}^2$$

382 because this provided a satisfactory visual setting for interpretation (the dispersion in
 383 the three dimensions is made the same; without affecting the volume of the tetrahedra).
 384 Figure 1(left) visualises the rank $R = 1$ approximation and shows how, by looking at
 385 tetrahedra, one can quickly get an impression of a specific triadditive interaction. Figure
 386 1(right) displays the visualisation for $R = 2$, via three biplots for the three factors. Each
 387 biplot may be visualised in one of the three orthogonal planes (uv , uw and vw) through
 388 the origin. The interaction of interest remains proportional to the volume of a single
 389 tetrahedron.

390 A three-dimensional rank $R = 3$ visualisation is crossing the line of useful application
 391 (as outlined in Section 3.2). It is much more simple to look at a two-dimensional
 392 visualisation through a so-called triplot. Here, we use the term triplot in the same

393 way as in Albers and Gower (2014). According to Williams and Gardner-Lubbe (2016),
 394 the use of the term ‘triplet’ in this context dates back to Araújo (2009). Meulman
 395 et al. (2004, p. 50) also use this term, in a slightly different context related to biplots.
 396 Furthermore, the term triplot is also used in for triangular diagrams, which is a unrelated
 397 field of work. As the contexts are fully different, this should not cause confusion.) In
 398 this display, each IJ combination of levels is represented by a calibrated axis while each
 399 level of K is represented by a point (for the Blackman data we have $I = 2$, $J = 7$ and
 400 $K = 12$). Thus, an axis combining a Site (e.g. Edinburgh) with the Higher Level of
 401 Nitrogen (e.g. denoted by H) might be labelled “Edinburgh H”. While another axis
 402 might be labelled “Edinburgh L”, where L denotes a Lower Level of Nitrogen. Because
 403 $I = 2$ the two Edinburgh axes coincide, as do the axes for all other sites.

404 Figure 6 displays such a triplot for the interaction array $\hat{\mathbf{Z}}$. All IJ combinations of
 405 nitrogen-rate and trial-site are displayed by calibrated axes but only $J = 7$, rather than
 406 $IJ = 14$, distinct axes are necessary. We use the convention that the label “Edinburgh”
 407 denotes not only the site but also the high rate of nitrogen. The marker for the low
 408 rate of nitrogen in Edinburgh could be placed at the other end of the axis but it is
 409 superfluous. The markers on the axis are positive in the section between the label (e.g.
 410 Edinburgh) and the origin and negative away from the origin; the opposite holds for the
 411 implicit Edinburgh \times low marker. All $K = 12$ varieties are displayed as points.

412 By projecting variety k onto the combined rate-site axes, triadic rank-two interactions
 413 can be read directly off the calibrations to give the estimation of the term for variety k
 414 and all combinations of levels of i and j . A ‘projection circle’ on the diameter determined
 415 by the point displaying the variety and through the origin, gives a convenient way of
 416 accessing all projections of the variety onto the $J = 7$ rate \times trial axes together with their
 417 associated calibrations. Such projection circles have been introduced in the context of
 418 biplots in Gower and Hand (1996) and Gower et al. (2011), and in the context of triplots
 419 in Albers and Gower (2014).

420 Figure 6 shows this visualisation for the Blackman data where the point ‘Cap’ rep-
 421 represents the variety Cappelle. Sites Begbroke, Trumpinton, and Earith give positive
 422 interactions, Boxworth about zero and sites Craftshill and Fowlmore give negative in-
 423 teractions between Cappelle and high levels of Nitrogen. The signs are reversed for
 424 interaction with low levels of Nitrogen. The intervals of calibration may be refined at
 425 will but here we give only a marker 10 grams per square meter. It is important to keep
 426 in mind when interpreting these triadic interactions that these are the values after main
 427 and biadditive effects (accounting for 98.07% of variation, see Table 2) have been par-
 428 tialed out: The triplot focuses on the remaining 1.93% of variation and large differences
 429 in the triplot denote, in this example, only relatively small differences on an overall level.

430 Note that (a) although this two-dimensional visualisation may look like a biplot it
 431 involves three factors and thus is really a triplot and (b) it remains valid when $I >$
 432 2, though without the simplifications of coincident axes, which might introduce visual
 433 overlaid. Both Albers and Gower (2014) and Williams and Gardner-Lubbe (2016) provide
 434 examples of such a triplot with $I = 3$.

435 5 Discussion

436 Essentially, our approach is to adopt the usual linear models for representing main effects,
 437 two factor interactions and three factor interactions. The two factor interactions may be
 438 approximated by multiplicative bilinear terms and the three factor interactions may be
 439 approximated by multiplicative trilinear terms. In the bilinear case the approximations
 440 have standard least-square estimates, based on singular value decompositions, but in the
 441 trilinear case, we propose that the estimates be conditioned on the residuals from the
 442 saturated bilinear model. In principal, it would be possible to do a full unconditional
 443 least-squares solution but the conditional approach is easier and avoids difficulties with
 444 constraints. In the bilinear case identification constraints are not substantive but in
 445 the full trilinear case there is a troubling substantive interaction between the bilinear
 446 and trilinear parameter constraints. This problem is avoided when using the conditional
 447 method of analysis. The suggestion of applying a triadditive model to three-way residuals
 448 has also been made by van Eeuwijk and Kroonenberg (1998), who used a Tucker3 model
 449 rather than the Candecomp-Parafac model. Williams and Gardner-Lubbe (2016) use an
 450 orthogonal Parafac decomposition as basis for their visualisations and arrive at figures
 451 similar to Figure 3(a) on basis of geometric arguments.

452 We do not claim that the biadditive and triadditive models are substantive models
 453 per se, although in certain applications they could be. We make use of biadditive and
 454 triadditive models as a useful framework to base our visualisations on. A special virtue
 455 of biadditive models is the way that they lend themselves to simple biplots for visu-
 456 alising the interactions between rows and columns of the two classifying factors. This
 457 is particularly useful when biadditive interactions are adequately approximated in two
 458 dimensions and in this paper we have proposed how these biplots may be enhanced. It
 459 would be helpful if similar visualisations were available for triadditive interactions and,
 460 following Albers and Gower (2014), we demonstrate how two-dimensional triplots for
 461 rank-two tridimensional interaction tables may be formed, in which all three-dimensional
 462 tetrahedral information is retained. When one factor is at two levels, some striking
 463 simplifications occur, as is demonstrated in Section 4). When $I, J, K > 2$, there is a

464 risk of visual overload. Such overload can be reduced through smart choices, construct-
465 ing parallel coordinate plots (such as Figure 5) for triplots and through interactivity.
466 For instance, markers for calibrated axes could be displayed only when a certain axis
467 is selected, and one could use tick boxes to select which of the IJ axes and K points
468 should be shown. Finding out which approaches work best against visual overload is an
469 interesting path for future research. Furthermore, additional smart choices w.r.t. cali-
470 bration, (arbitrary) rotation and use of colour can enhance the interpretability (Blasius
471 et al., 2009).

472 Rank two triplot displays in two dimensions seem to be at the bounds of practical
473 utility. Attempts to visualise rank-three displays in three dimensions are not promising.
474 Fortunately, as with biadditive biplots, it is the rank-two displays that are the most
475 useful and rank two tridimensional visualisations show similar promise.

476 At the outset of this paper we drew attention to the adage of McCullagh and Nelder
477 about interactions being predicated on their main effects and lower orders of interaction.
478 Our approach of conditioning three-order interactions on main effects and two-factor in-
479 teractions is in accord with the adage. Nevertheless, at several points in our discussion
480 we have seen that main effects and lower order interactions may be ignored when fitting
481 a higher-order interaction. Sometimes, but not always, it seems that, as with Tukey's
482 model of non-additivity, additive terms may be absorbed in equivalent multiplicative
483 parameterisations of the model. It seems to us that it is always wise to keep the McCul-
484 lagh and Nelder adage in mind but there are occasions, especially with multiplicative
485 relationships, when it is less persuasive.

486 **Software**

487 All computations have been performed in R, using self-written code (available upon re-
488 quest from the first author). For the Candecomp-Parafac decompositions the R-package
489 `ThreeWay` (Giordani et al., 2014) has been used. For the correspondence analyses, the
490 R-package `ca` (Nenadic and Greenacre, 2007) has been used.

491 **Acknowledgements**

492 Dr. Steffen Unkel (University of Göttingen, Germany) gave helpful comments on Section
493 2. The attendants of the TRICAP 2015 conference, Prof. Pieter Kroonenberg (Leiden
494 University, The Netherlands) and Dr. Sugnet Lubbe (University of Cape Town, South
495 Africa) in particular, provided valuable feedback.

496 Appendices

497 A Calibrated biplots for biadditive interaction arrays

498 In the notation of Section 2.1 it is useful, especially when $R = 2$, to plot the rows of \mathbf{c}_r
 499 ($r = 1, \dots, I$) to give I row-points and the rows of $\tilde{\mathbf{c}}_s$ ($s = 1, \dots, J$) to give J column-
 500 points. In this biplot, the inner-product determined by a pair of points, one from each
 501 set, gives a visualisation of the corresponding interaction. Here \mathbf{c}_r and $\tilde{\mathbf{c}}_s$ derive from
 502 the SVD of $\mathbf{X} = \mathbf{U}\mathbf{\Sigma}\mathbf{V}'$ and we set $\mathbf{c}_r = \mathbf{u}_r\mathbf{\Sigma}^\alpha$ and $\tilde{\mathbf{c}}_s = \mathbf{v}_s\mathbf{\Sigma}^\beta$ where usually $\alpha + \beta = 1$.

503 If we project $\tilde{\mathbf{c}}_s$ onto the vector \mathbf{c}_r we find $\left[\mathbf{\Sigma}^\beta\mathbf{v}'_s(\mathbf{v}_s\mathbf{\Sigma}^{2\beta}\mathbf{v}'_s)^{-1}\mathbf{v}_s\mathbf{\Sigma}^\beta\right]\mathbf{\Sigma}^\alpha\mathbf{u}'_r$ which,
 504 when $\alpha + \beta = 1$ simplifies to

$$\left[\mathbf{\Sigma}^\beta\mathbf{v}'_s(\mathbf{v}_s\mathbf{\Sigma}^{2\beta}\mathbf{v}'_s)^{-1}\right]\mathbf{v}_s\mathbf{\Sigma}\mathbf{u}'_r = \left[\mathbf{\Sigma}^\beta\mathbf{v}'_s(\mathbf{v}_s\mathbf{\Sigma}^{2\beta}\mathbf{v}'_s)^{-1}\right]z_{rs}. \quad (\text{A1})$$

505 In (A1), only the interaction z_{rs} depends on r so all points $r = 1, \dots, I$ are collinear
 506 on an axis with direction given by the term of (A1) given in square brackets. It follows
 507 that $\left[\mathbf{\Sigma}^\beta\mathbf{v}'_s(\mathbf{v}_s\mathbf{\Sigma}^{2\beta}\mathbf{v}'_s)^{-1}\right]$ may be used to calibrate the axis with values $\mu_1, \mu_2, \mu_3, \dots$
 508 usually chosen with an even calibration interval κ as $\mu, \mu \pm \kappa, \mu \pm 2\kappa, \dots$. Setting $\mu = 0$
 509 gives the scale for $z_{\mu s}$. If we set $\mu = a_r$ the markers include the main effect of the i th
 510 main effect a_r , so giving the combined effects of the main effect and interactions of r
 511 with all the columns s . Note that this merely requires a cosmetic change to the markers
 512 and not any extra calculation.

513 Similarly, all rows $r = 1, 2, \dots, I$ may be shown as calibrated axes and if we project
 514 \mathbf{c}_r onto the vector $\tilde{\mathbf{c}}_s$ all columns $s = 1, 2, \dots, J$ may be shown as axes calibrated in
 515 terms of $\left[\mathbf{\Sigma}^\alpha\mathbf{u}'_r(\mathbf{u}_r\mathbf{\Sigma}^{2\alpha}\mathbf{u}'_r)^{-1}\right]$.

516 Note that the marker for z_{rs} occurs twice, once on \mathbf{c}_r and once on $\tilde{\mathbf{c}}_s$. Furthermore,
 517 the distances of the two markers from the origin are unequal. It would be elegant to
 518 arrange equal scaling but we have not succeeded and believe it to be impossible.

519 B Automatic ordering of the parallel axes

520 In constructing parallel coordinate plots as Figures 4 and 5, the ordering of the axes
 521 usually is irrelevant (unless the corresponding factor is at some ordinal level). In that
 522 case, visual information might be gained by rearranging the axes optimally.

523 In total, $J!$ orderings are possible and, by excluding mirrorings ('ABCD' yields the
 524 same information as 'DCBA'), there are $J!/2$ orderings to choose between.

525 This appendix explains an automated procedure to do so, based on correspondence

526 analysis (CA). CA is similar to principal component analysis, but for nominal-labelled
527 data.

528 Let \mathbf{Y} be the $J \times K$ table with the projections for the K varieties on the J sites (either
529 with or without main effects). The goal is to rearrange the J columns optimally; i.e.
530 such that projections on adjacent axes are as close as possible. Since correspondence
531 analysis is designed for non-negative data, we shift \mathbf{Y} such that all values are non-
532 negative, i.e. through $\mathbf{Y}' = \mathbf{Y} - \min \mathbf{Y}$. Since the row sums of \mathbf{Y} are zero (since the
533 average interaction per site is zero), and hence the row sums of \mathbf{Y}' are equal, some
534 simplifications with respect to general correspondence analysis are possible, although
535 the gain in computation speed is negligible for small values of J (such as in Section 4).

536 The simplified algorithm is as follows:

- 537 1. Compute $\mathbf{M} = \mathbf{S} - \mathbf{w}_J \mathbf{w}'_K$, where $\mathbf{S} = \mathbf{Y}' / \sum \sum y'_{jk}$, \mathbf{w}_J is the $J \times 1$ vector
538 of row weights with equal entries $1/J$, and \mathbf{w}_K is the $K \times 1$ vector with entries
539 $\sum_j y'_{jk} / \sum_{jk} y'_{jk}$;
- 540 2. Perform a SVD on \mathbf{M} : $\mathbf{M} = \mathbf{U} \mathbf{\Sigma} \mathbf{V}'$ under the restrictions $\mathbf{U}' \mathbf{U} = \mathbf{J} \mathbf{I}$ and
541 $\mathbf{V}' \text{diag}(\mathbf{w}_K) \mathbf{V} = \mathbf{I}$;
- 542 3. Compute $\mathbf{F}_J = \mathbf{U} \mathbf{\Sigma}$;
- 543 4. Rearrange the J rows of \mathbf{Y} according to the ordering in the first column of \mathbf{F}_J .

544 In Step 4, one could rearrange the rows ascending or descending, which yields two
545 visualisations that are one another's mirror image.

546 References

- 547 C. J. Albers and J. C. Gower. A contribution to the visualisation of three-way arrays.
548 *Journal of Multivariate Analysis*, 132:1–8, 2014.
- 549 C. J. Albers, J. C. Gower, and H. A. L. Kiers. Rank properties for centred three-
550 way arrays. In F. Mola, C. Conversano, and M. Vichi, editors, *Classification, (Big)*
551 *Data Analysis and Statistical Learning*, Studies in Classification, Data Analysis, and
552 Knowledge Organization. New York: Springer, 2017.
- 553 L. Araújo. Seleção e análise dos modelos PARAFAC e Tucker e gráfico triplot com
554 aplicação em interação tripla. doctoral thesis. university of Sao Paulo, Brazil, 2009.

- 555 J. A. Blackman, J. Bingham, and J. L. Davidson. Response of semi-dwarf and con-
556 ventional winter wheat varieties to the application of nitrogen fertilizer. *Journal of*
557 *Agricultural Science*, 90:543–550, 1978.
- 558 J. Blasius, P. H. C. Eilers, and J. C. Gower. Better biplots. *Computational Statistics*
559 *and Data Analysis*, 53:3145–3158, 2009.
- 560 R. Bro and M. Jakobsen. Exploring complex interactions in designed data using GE-
561 MANOVA. color changes in fresh beef during storage. *Journal of Chemometrics*, 16
562 (6):294–304, 2002. doi: 10.1002/cem.722.
- 563 J. D. Carroll and P. Arabie. Multidimensional scaling. *Annual Review of Psychology*,
564 31:607–649, 1980.
- 565 J. D. Carroll and J. J. Chang. Analysis of individual differences in multidimensional
566 scaling via an n -way generalization of ‘Eckart-Young’ decomposition. *Psychometrika*,
567 35:283 – 319, 1970.
- 568 C. Coombs. *A theory of data*. New York: John Wiley, 1964.
- 569 L. C. A. Corsten and A. C. Van Eijnsbergen. Multiplicative effects in two-way analysis
570 of variance. *Statistica Neerlandica*, 26:61–68, 1972.
- 571 J. B. Denis and J. C. Gower. Biadditive models. *Biometrics*, 50:310 – 311, 1994.
- 572 M. d’Ocagne. *Coordonnées parallèles et axiales: Méthode de transformation géométrique*
573 *et procédé nouveau de calcul graphique déduits de la considération des coordonnées*
574 *parallèles*. Paris: Gauthier-Villars, 1885.
- 575 H. D. Gauch. *Statistical analysis of regional yield trials: AMMI Analysis of Factorial*
576 *Designs*. Amsterdam: Elsevier, 1992.
- 577 P. Giordani, H. A. L. Kiers, and M. A. del Ferraro. Three-way component analysis using
578 the R package ThreeWay. *Journal of Statistical Software*, 57, 2014.
- 579 H. F. Gollob. A statistical model that combines features of factor analytic and analysis
580 of variance techniques. *Psychometrika*, 33:73–115, 1968.
- 581 J. C. Gower. The analysis of three-way grids. In P. Slater, editor, *Dimensions of Intra*
582 *Personal Space, vol. 2, The Measurement of Intra Personal Space by Grid Technique*,
583 pages 163–173. Chicester: Wiley, 1977.
- 584 J. C. Gower and D. J. Hand. *Biplots*. London: Chapman and Hall, 1996.

- 585 J. C. Gower, P. J. F. Groenen, and M. van de Velden. Area biplots. *Journal of Computational and Graphical Statistics*, 19:46 – 61, 2010.
- 586
- 587 J. C. Gower, S. Lubbe, and N. Le Roux. *Understanding biplots*. Chichester: Wiley, 2011.
- 588 M. Greenacre. *Correspondence analysis in practice*. London: Chapman & Hall, second
589 edition, 2007.
- 590 R. A. Harshman. Foundations of the PARAFAC procedure: Models and methods for an
591 ‘explanatory’ multi-mode factor analysis. *UCLA Working Papers in Phonetics*, 16:1
592 84, 1970.
- 593 A. I. Inselberg. *Parallel Coordinates: Visual Multidimensional Geometry and its Appli-*
594 *cations*. Springer, 2009.
- 595 H. A. L. Kiers. Towards a standardized notation and terminology in multiway analysis.
596 *Journal of Chemometrics*, 14:105–122, 2000.
- 597 P. M. Kroonenberg. *Applied Multiway Data Analysis*. Hoboken, New Jersey: Wiley,
598 2008.
- 599 P. M. Kroonenberg and T. H. A. van der Voort. Multiplicatieve decompositie van
600 interacties bij oordelen over werkelijkheidswaarde van televisiefilms. *Kwantitatieve*
601 *methoden*, 8:117–144, 1987.
- 602 P. McCullagh and J. A. Nelder. *Generalized Linear Models*. Boca Raton, Florida:
603 Chapman & Hall/CRC, 2nd edition, 1989.
- 604 J. J. Meulman, A.J. van der Kooij, and W. J. Heiser. Principal components analysis
605 with nonlinear optimal scaling transformations for ordinal and nominal data. In
606 D. Kaplan, editor, *The SAGE handbook of quantitative methodology for the social*
607 *sciences*. London: Sage, 2004.
- 608 O. Nenadic and M. Greenacre. Correspondence analysis in R, with two- and three-
609 dimensional graphics: the ca package. *Journal of Statistical Software*, 20, 2007.
- 610 C. R. Rao. *Advanced Statistical Methods in Biometric Research*. New York: John Wiley
611 & Sons, 1952.
- 612 E. Schmidt. Zur theorie der linearen und nichtlinearen Integralgleichungen. 1. Teil:
613 Entwicklung willkürlicher Funktionen nach System vorgeschriebener. *Mathematische*
614 *Annalen*, 63:433 – 476, 1907.

- 615 A. K. Smilde, R. Bro, and P. Geladi. *Multi-way analysis with applications in the chemical*
616 *sciences*. Hoboken, New Jersey: John Wiley & Sons, 2004.
- 617 J. M. F. ten Berge. Simplicity and typical rank results for three-way arrays. *Psychome-*
618 *trika*, 76:3 – 12, 2011.
- 619 M. E. Timmerman and H. A. L. Kiers. Three-mode principal component analysis:
620 choosing the numbers of components and sensitivity to local optima. *British Journal*
621 *of Mathematical and Statistical Psychology*, 53:1–16, 2000.
- 622 L. R Tucker. Some mathematical notes in three-mode factor analysis. *Psychometrika*,
623 31:279–311, 1966.
- 624 J. W. Tukey. One degree of freedom for non-additivity. *Biometrics*, 5:232–242, 1949.
- 625 F. A. van Eeuwijk and P. M. Kroonenberg. Multiplicative models for interaction in
626 three-way ANOVA, with applications to plant breeding. *Biometrics*, 54:1315 – 1333,
627 1998.
- 628 D. Williams and S. Gardner-Lubbe. Visualising three-way arrays. *Chemometrics and*
629 *Intelligent Laboratory Systems*, 158:180–186, 2016.

630 **Tables**

Trial site	abbreviation
Craftshill	Cra
Begbroke	Beg
Fowlmere	Fow
Trumpington	Tru
Boxworth	Box
Earith	Eea
Edinburgh	Edi

Variety	abbreviation
Cappelle	Cap
Ranger	Ran
Huntsman	Hun
Templar	Tem
Kinsman	Kin
Fundin	Fun
Durin	Dur
Hobbit	Hob
Sportsman	Spo
TJB259.95	259
TJB325.464	325
Hustler	Hus

Table 1: Overview of the trial sites (left) and varieties of wheat (right) of the Blackman data set, as well as the abbreviations used in later visualisations.

Factor	SS	df	% of total
A (rate of nitrogen application)	125078	1	4.84
B (trial site)	1854207	6	71.72
C (variety of wheat)	196211	11	7.59
AB	221481	6	8.57
AC	8021	11	0.31
BC	130411	66	5.04
$r = 1$	60961	(16)	
$r = 2$	42642	(14)	
$r = 3$	12623	(12)	
$r = 4$	8334	(10)	
$r = 5$	3799	(8)	
$r = 6$	2053	(6)	
ABC	49812	66	1.93
Total	2585224	167	

Table 2: ANOVA-breakdown of Blackman's data. The SS for the rows with specific values for r are obtained via (7). The corresponding degrees of freedom are obtained via the rule of thumb explained in Section 2.2. (Note that, since $df_A = 1$, no similar breakdown for the AB and AC interaction is possible.)

Rank S	Fit (%)	Increment
1	35.40	35.40
2	63.10	27.70
3	78.62	15.52
4	88.89	10.27
5	97.74	8.85
6	100.00	2.26

Table 3: Candecomp-Parafac approximations to the three-way interaction ABC for different ranks S for Blackman's data.

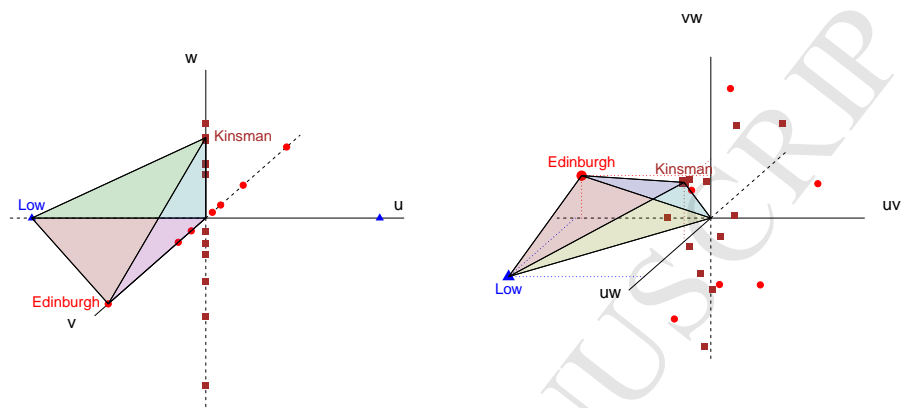
631 **Figures**

Figure 1: Rank $R = 1$ (left) and $R = 2$ (right) fits to the triadditive terms for Blackman's data. Blue triangles refer to Factor A (the levels of nitrogen), red circles to Factor B (trial sites) and brown squares to Factor C (varieties). For the $R = 1$ fit, all points lie on orthogonal axes, for the $R = 2$ fit, they all lie on orthogonal planes. The tetrahedra corresponds to the interaction "low nitrogen \times Edinburgh \times Kinsman".

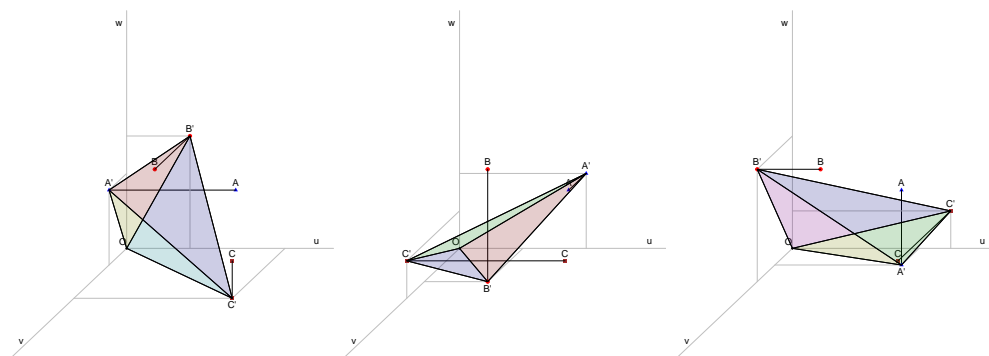


Figure 2: A demonstration of a three-way interaction for the rank $R = 3$ fit to triadditive terms, for a constructed example with conveniently chosen coordinates. All levels of all factors now have coordinates that are not restricted to (orthogonal) axes nor planes. The three points A, B, C , are projected onto the vw, uw and uv planes, respectively. Subsequently, the polygon $OA'B'C'$ is constructed (left). Similarly, polygons are constructed for projections onto uw, uv and vw (middle) and uv, vw and uw (right). The interaction ABC is proportional to the sum of the volumes of the three tetrahedra thus obtained.

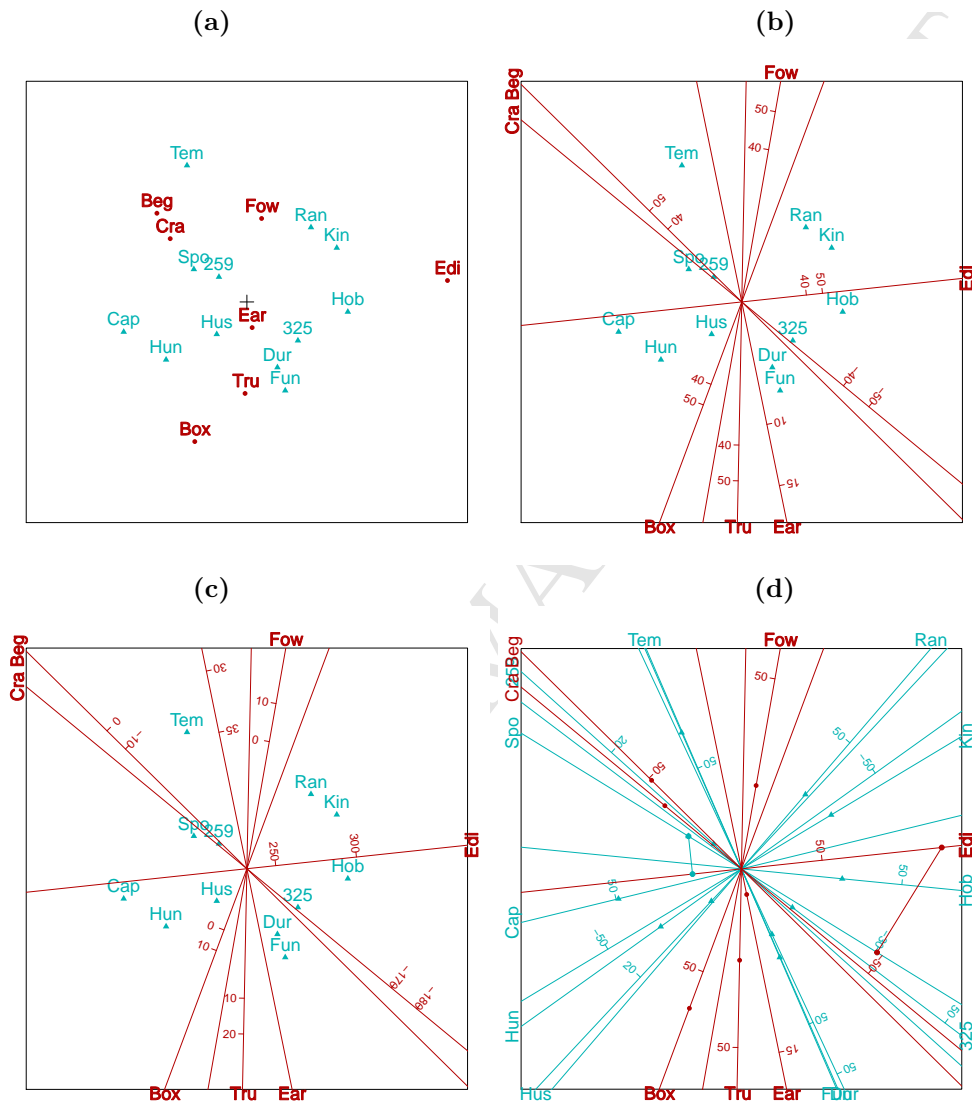


Figure 3: Visualisation of the rank $R = 2$ approximation to the biadditive interaction between factors B and C. First (a) a regular biplot is given (with + indicating the origin; trial locations are denoted by ‘.’ and varieties by a triangle), followed by a biplot where trial sites have been replaced by calibrated axes; where calibration is done with $\mu = 0$ (b) and $\mu = b_j$ (c). Finally, panel (d) shows a biplot where both varieties and trial sites are represented by calibrated axes. Abbreviations in bold font correspond to trial sites. See Table 1 for the full labels for the abbreviations.

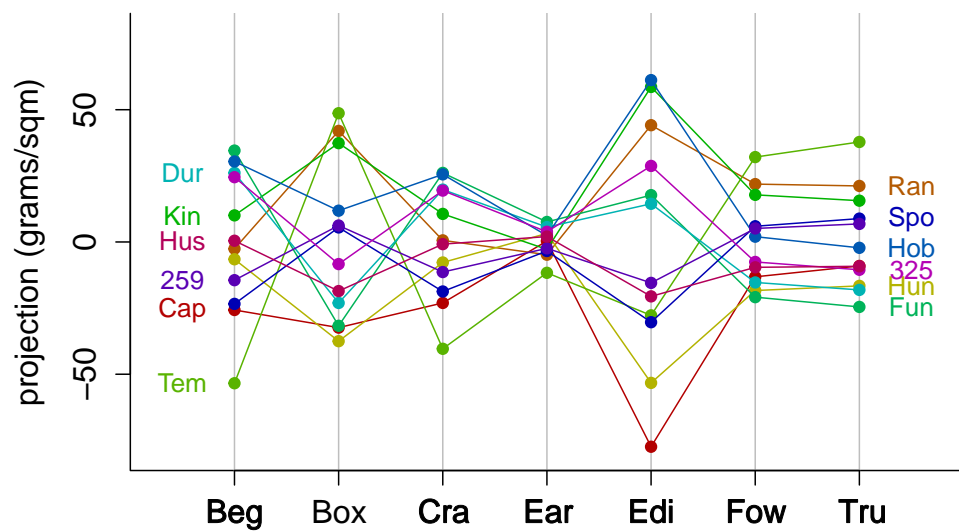


Figure 4: For all 7 trial sites the projections of the varieties (with $\mu = 0$) are given in this single-axis diagram. A single calibrated axis applies to all sites. Abbreviations in bold font correspond to trial sites. See Table 1 for the full labels for the abbreviations.

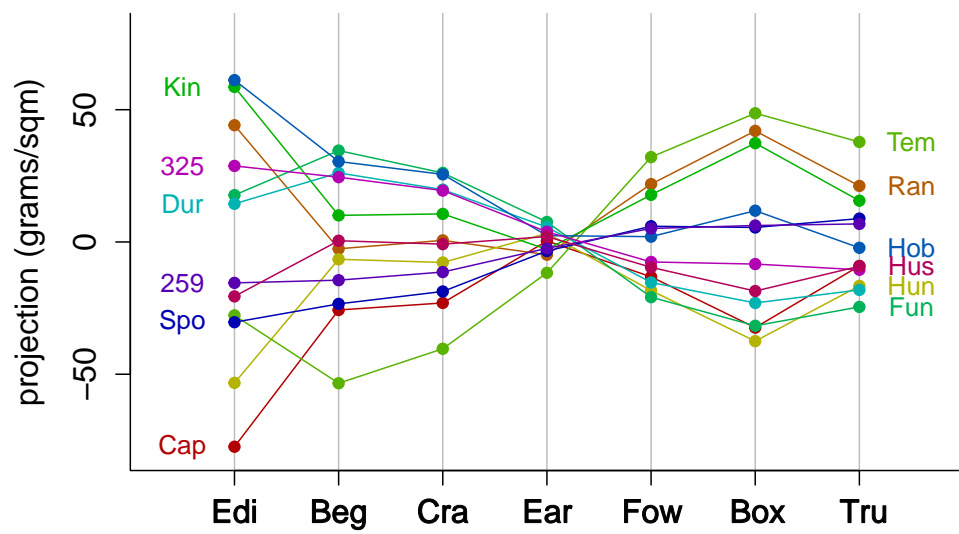


Figure 5: A similar visualisation as Figure 4, now with the ordering of sites according to the correspondence analysis algorithm outlined in Appendix B.

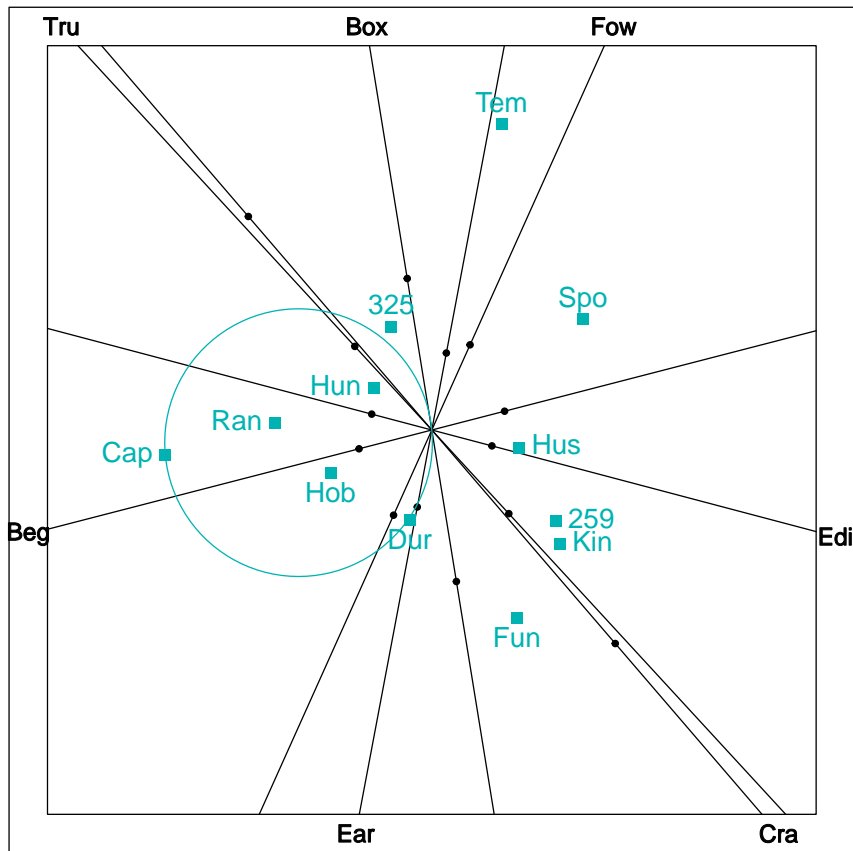


Figure 6: Triplot. Axes represent rates and sites. Since $I = 2$, the axes for low and high rates coincide. Site labels are placed at the positive end of the 'high'-axis. The signs are reversed for predicting interactions to the low rate of nitrogen. A single positive and negative marker is shown on each axes; these correspond to 10 grams per square meter grain yield. A projection circle through Cappelle cuts the axes at the calibrations corresponding to the seven calibration points giving the rank-two triadic interactions. These are positive or negative, depending on whether they occur on the same or opposite side of the origin as the site label. Abbreviations in bold font correspond to trial sites. See Table 1 for the full labels for the abbreviations.